RADIATION CHARACTERISTICS OF SOLID RECTANGULAR DIELECTKIC HORNS

R Chatterjee, K G Narayanan, and A Kumar

ABSTRACT

The radiation characteristics of solid dielectric horns of rectangular cross-section, excited by a rectangular metal waveguide operating in the dominant TE_{10} mode, have been studied both theoretically and experimentally. The theoretical analysis is based on the modal knowledge of the field distributions around the dielectric structure and over the free-end aperture. The effect of the feed-end radiation is superposed suitably on the free-end radiation to obtain the total far-field pattern. Experimental verification of the theoretical results is obtained by probing the near-field as well as by the measurement of the far-field pattern at λ = 3.2 cm and λ = 3.2 mm.

1. INTRODUCTION

Dielectric rods of rectangular cross-section have been receiving greater attention in recent times with the advent of planar millimeter wave integrated circuits and of integrated optics. Several applications as radiators and waveguide components have been aeveloped. Light weight dielectric antennas of rectangular cross-section have been studied by Kobayashi et al (1), Sen and Chatterjee (2), Paulit ana Chatterjee (3) and others. Radiation from pyramidal dielectric waveguides has been studied by Brooking et al (4). In this paper is presented the results of an analytical and experimental study of the guidance and radiation characteristics of solid dielectric rectangular horns carrying the E^y_{11} mode.

2. GUIDED MODES IN THE RECTANGULAR SOLID DIELECTRIC HORN

The boundary-value problem of the rectangular solid dielectric horn (Fig. 1) has been studiea by modelling it as a cascade of piecewise uniform rectangular dielectric guides (Fig. 2). Using Marcateli's *(4)* method, the following characteristic equations have been derived for E^y_{pq} modes:

$$k_x = (p\pi/a) - (2/a)\tan^{-1}\left[(\mu_2/\mu_1)(k_x/k_{x_2})\right] \quad (1)$$

$$k_y = (q\pi/b) - (2/b)\tan^{-1}\left[(\epsilon_2/\epsilon_1)(k_y/k_{y_3})\right] \quad (2)$$

where k_x, k_{x2} and k_y, k_{y2} are the propagation constants in the x and y directions inside the uielrctric rod and in regions (2,4) and (3.5). Similarly the characteristic equations for E^x_{pq} modes are

$$k_x' = (2p\pi/a) - (2/a)\tan^{-1}\left[(\epsilon_2/\epsilon_1)(k_x'/k_{x_2}')\right] \quad (3)$$

$$k_y' = (2q\pi/b) - (2/b)\tan^{-1}\left[(\mu_2/\mu_1)(k_y'/k_{y_3}')\right] \quad (4)$$

For hybrid modes, eqs. (1), (2), (3) and (4) all hold *good.* The transverse and longitudinal propagation constants have been obtained by solving the characteristic equations graphically and numerically for horns of small flare angles upto 60°. Fig. (3) shows the theoretical and experimental variation of Ey over the free-end aperture of a pyramidal horn antenna and Fig. (4) the theoretical and experimental variation of k_z along the length of the horn for another pyramidal horn antenna for the E^y_{11} mode. It can be seen that the agreement between theory and experiment is good.

Calculation of the average power flowing down the horn inside and outside, shows that less than 5% of the total power flows outside the horn, when the length of the horn exceeds about 5 . Fig. 5 shows the calculated power confinement versus length for an X-band horn and a 95 GHz band horn.

The measured phase error over the free end of the horn is less thzn 25° for small angle horns; hence the assumption of a plane wave propagating along the axial direction in the horn is satisfactory. For aperture dimensions greater than 3 , the phase error increases and hence the propagating wave becomes more spherical.

3. THEORETICAL RADIATION CHARACTERISTICS

The two-aperture theory used by Brown and Spector (5) and by James (6) has been used to derive the radiation characteristics of the rectangular solid dielectric horn. The horn is assumed to be an efficient surface waveguide to transport all the energy launched into it in the form of guided modes upto the free end from where it is radiated. Some energy which fails to be trapped by the total internal reflection phenomenon in the guide is radiated out of the dielectric structure close to the feed end and interferes with the free-end radiation at the far field.

3.1 Radiation due to the Free-end Aperture

The radiation field due to the fields distributed tangentially over the free-end aperture plane of the dielectric horn is ootained by the scalar diffraction integral. The diffracted field at any point P due to a distribution of fields on an aperture is given by Silver (7).

$$U_p = \frac{1}{4\pi}\int_A F(x,y)\exp(-jk_0 r)/r\left[(j k_0 + \frac{1}{r})\vec{i}_z \cdot \vec{r}_1 + jk_0 \vec{i}_z \cdot \vec{s}\right] dx\,dy \quad (5)$$

where $F(x,y) = A(x,y)\exp[-j\psi(x,y)]$ $A(x,y)$ being the amplitude distribution and $\psi(x,y)$ the phase distribution over the aperture A, $\vec{R}$ is the unit vector in the direction of the field point P from the point (x,y) on the aperture plane, and $\vec{s}$ is the unit vector normal to the wave front at the aperture plane towards P.

The phase $\psi(x,y)$ at the point (x,y,z_t) on the free-end aperture plane $z = z_t$ is given by

$$\psi(x,y) = \int_0^{R_s} k_z \, dR_s = (1/\cos\theta_s)\int_0^{z_t} k_z \, dz \qquad (6)$$

where

$$\theta_s = \tan^{-1}\left|(x^2+y^2)^{1/2}/z_t\right| \qquad (7)$$

R_s being the radial distance from the origin to the point (x,y,z), if the distribution of phase over the aperture is assumed to be that corresponding to the Presence of a spherical wave at this plane, in a manner similar to the treatment of a small metallic horn as given by Collin and Zucker (8). Eq. (6) is used in evaluating eq. (5).

3.2 Radiation due to the Feed-end

The radiation from the feed-end is assumed to be that of the open-ended rectangular metal wave-guide launcher, as modified by the presence of the dielectric in front of it. A relative amplitude weighting factor which gives the best fit with the experimentally observed pattern is determined by a trial and error method, and this is used while superposing the feed-end radiation and the free-end radiation. If the power flow in the launcher metal waveguide carrying the TE_{10} mode is P_L, the power flow in the rectangular dielectric guide propagating in the EY_{11} mode is P_D, and if the power that can be radiated out of the free-end plane is P_T, then

$$P_T = (1-\Gamma)(1-\alpha)P_D \qquad (8)$$

where Γ = power reflection coefficient at the feed-end and α is the fraction of the total power P_L that escapes the dielectric guide by radiation at the feed-end junction. The maximum value P_{Tmax} of P_T is given by

$$P_{Tmax} = P_D = P_L \qquad (9)$$

Using eq. (9), the maximum ratio of the field amplitude coefficient C_1 of the EY_{11} mode to the field amplitude coefficient A_{10} of the TE_{10} mode can be evaluated. This ratio (C_1/A_{10}) has to be reduced to obtain the best match of the theoretical radiation pattern with the experimental pattern, when the feed-end and free-end radiation patterns are superimposed to obtain the total radiation pattern.

Due to refraction effects at the boundary surfaces of the dielectric horn, the radiation from the feed-end is modified in two ways as follows: (a) The direction of the emergent ray is modified and this shifts the angular pattern of the feed aperture (b) The amplitude of the fields emerging out of the dielectric is modified differently in different directions, according to the Fresnel refraction coefficient. Quantitatively, this results in the necessity of multiplying the Original feed-end radiation pattern in the $\phi = 0^o$ and $\phi = 90^o$ planes by the factors T_s and T_p respectively as given by Narayanan(9).

4. EXPERIMENTAL

The observed radiation patterns of rectangular solid dielectric horns excited by a simple open ended metal waveguide launcher have a characteristic side-lobe structure with spaced minima resulting from the interference effects of the feed-end radiation and the free-end radiation.

The patterns are fairly similar in the E and H planes. The maximum gain is about 6 db. The cross-polarized field components are quite small. The positions of the first few minima and the gain along the boresight direction are sensitive functions of the flare angle of the horn, for a given horn length. These characteristics suggest the possibility of utilizing such antennas in specialized applications.

Fig. 6 and 7 show experimental and theoretical radiation patterns of two horns at $\lambda = 3.2$ cm and $\lambda = 3.2$ mm respectively.

5. CONCLUSIONS

The agreement between theory and experiment is good. The assumption of the EY_{11} mode at the terminal plane gives satisfactory results for the radiation patterns of small angle horns, while it is necessary to consider higher order modes for large aperture horns.

REFERENCES

1. Kobayashi, S. et al, 1982, 'Dielectric tapered rod antennas for millimeter-wave applications', IEEE Trans. Ant. and Prop., Vol. AP-30, No.1, pp. 52-58.

2. Sen, T.K. and Chatterjee, R., 1978, 'Rectangular dielectric rod at microwave frequencies - Parts I and II', J. Ind. Inst. Sci., Vol. 60, No.5, pp. 193-225.

3. Paulit, S.K. and Chatterjee, R., 1983, 'Radiation characteristics of tapered rectangular dielectric rod antennas at microwave frequencies', 1983 URSI International Symposium on Antennas and Propagation, Santiago de Compostela, Spain, pp. 23-26.

4. Brooking. N. et al, 1974. 'Radiation patterns of pyramidal dielectric wave-guides', Electronics Lett., Vol. 10, No. 3, pp. 33-34.

5. Brown, J. and Spector, J.O., 1957, 'The radiating properties of end-fire aerials; Proc. IEE, Vol. 104 B, pp. 27-34.

6. James. J.R., 1967, 'Theoretical investigations of cylindrical dielectric antennas'. Proc. IEE, Vol. 114, No.3, pp. 309-319.

7. Silver, S., 1949, 'Microwave Antenna Theory and Design', Radiation Laboratory Series, McGraw Hill, pp 158-162, and pp. 226-227.

8. Collin, R.E. and Zucker, F.J. 1966, 'Antenna Theory, Part II', McGraw Hill, Chap. 21.

9. Narayanan, K.G., 1984, 'Radiation characteristics of rectangular dielectric horn antennas', Ph.D. Thesis, Ind. Inst. Sci., Bangalore, India.

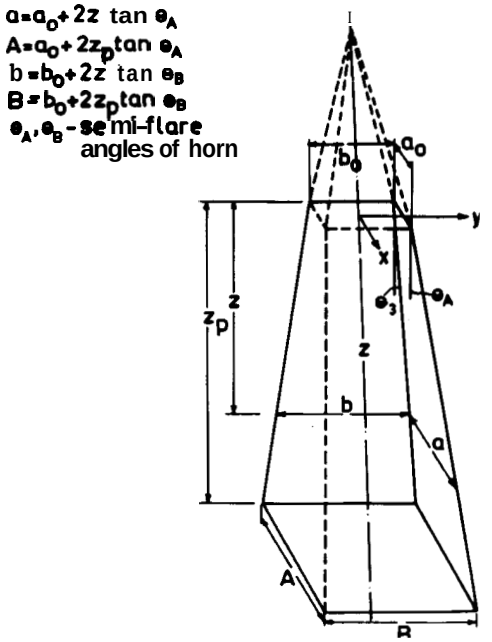

FIG.I RECTANGULAR DIELECTRIC HORN GEOMETRY

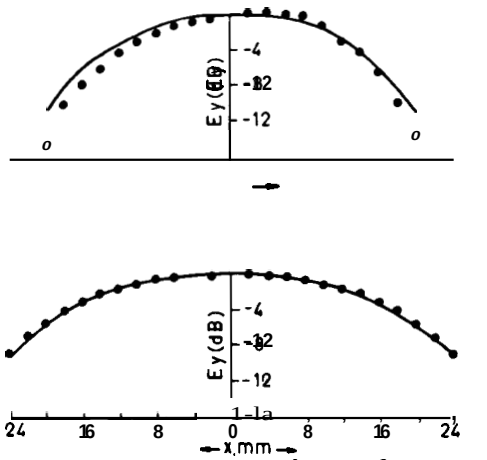

(b)Pyramidal horn θ_A=2·5°, θ_B=2·5°, L=35cm

ϵ_r=2·56, λ=3.2cm. a_0=2.28cm, b_0=1.0 cm

— Theory E_{11}^y • Measured

FIG.3.VARIATION OF E_y OVER FREE-END APERTURE

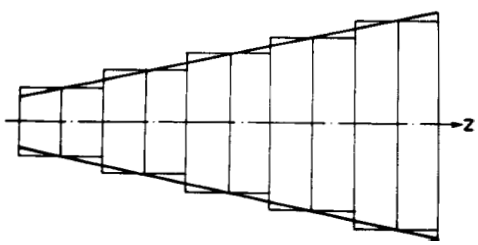

FIG.2a. APPROXIMATION OF DIELECTRIC HORN BY CASCADED UNIFORM GUIDES

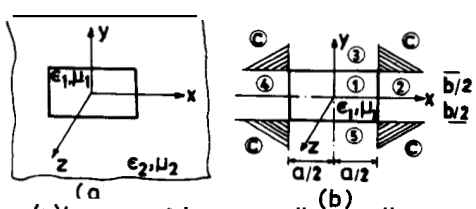

(a)Immersed in surrounding medium

(b)Regions of field distribution

FIG.2b. RECTANGULAR DIELECTRIC GUIDE IN CROSS SECTION

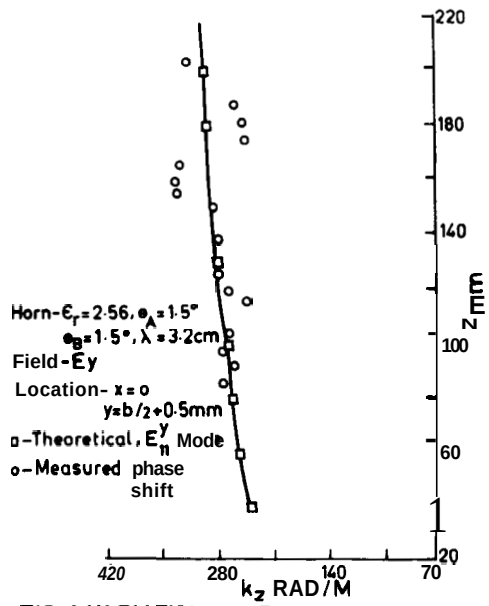

FIG.4.VARIATION OF FIELDS & k_z ALONG THE LENGTH OF THE HORN (PYRAMIDAL)

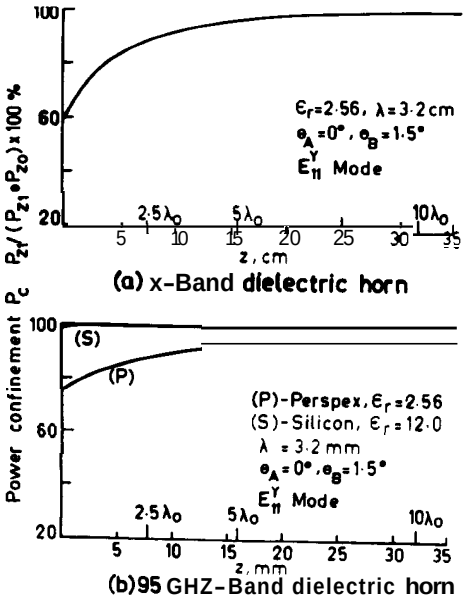

(a) x-Band dielectric horn

(b) 95 GHZ-Band dielectric horn

FIG.5. POWER FLOW IN RECTANGULAR DIELECTRIC HORNS

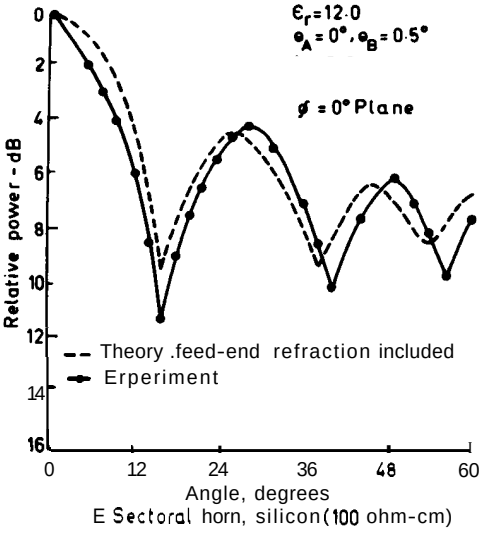

E Sectoral horn, silicon (100 ohm-cm)

FIG.7. RADIATION PATTERNS OF DIELECTRIC HORNS AT 95 GHZ BAND.

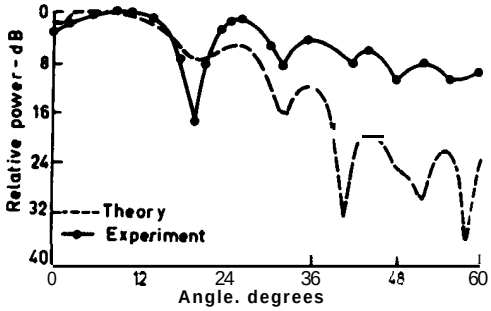

ϵ_r=2·56 , θ_A=2·5°
λ =3·2cm, θ_B=2·5°
L = 30.0 cm, ϕ =0° Plane
Feed-end refraction included

FIG.6. RADIATION PATTERN OF RECTANGULAR DIELECTRIC HORNS